Anisotropic Schrödinger Equation Quantum Corrections for 3D Monte Carlo Simulations of Nanoscale Multigate Transistors

M. A. Elmessary*†, D. Nagy*, M. Aldegunde‡, J. Lindberg *, W. Dettmer*,
D. Perić*, A. Loureiro*, and K. Kalna*
*College of Engineering, Swansea University, Swansea SA2 8PP, Wales, United Kingdom
†Dept of Mathematics & Engineering Physics, Faculty of Engineering, Mansoura University, Mansoura, Egypt
‡WCPM, School of Engineering, University of Warwick, Coventry CV4 7AL, England, United Kingdom
Phone: +44 1792 602816, Fax: +44 1792 295676, Email: M.A.A.Elmessary.716902@swansea.ac.uk

Multi-gate FETs like FinFETs and GAA nanowire (NW) are leading solutions for sub-10 nm technology because of their superior electrostatic integrity [1]. However quantum confinement and the complex 3D device geometry need to be realistically modelled for accurate physical simulations of carrier transport.

Here, we report on anisotropic finite element (FE) Schrödinger equation based quantum corrections (SEQCs) for our in-house 3D FE Monte Carlo (MC) device toolbox [2], [3]. The MC has already anisotropic bandstructure using **k**-vector transformations [4] but the Schrödinger equation QCs [5] were approximated by isotropic electron effective mass tensor (EMT) [2]. We extend the calibration-free Schrödinger equation QCs into three Δ valleys using longitudinal and transverse electron effective masses. Table I collects the EMT of Si Δ valley for $\langle 100 \rangle$ and $\langle 110 \rangle$ channel orientations. The 3D device FE mesh contains predefined 2D planes perpendicular to the transport direction, that are used to obtain the 2D potential for 2D Schrödinger equation [6]: $-\frac{\hbar^2}{2}\nabla_\perp \cdot \left[(\mathbf{m}^*)^{-1} \cdot \nabla_\perp \psi(y,z)\right] + U(y,z)\psi(y,z) = E\psi(y,z)$, where E is the energy, $(\mathbf{m}^*)^{-1}$ is the inverse EMT with components define as $(\mathbf{m}^*_{ij})^{-1} = \omega_{ij}$, $i,j = y,z$; $\psi(y,z)$ is the wavefunction penetrating into surrounding oxide, and $U(y,z) = -[qV(y,z) + \chi(y,z)]$ is the potential energy with $\chi(y,z)$ being the electron affinity [2]. The Schrödinger Eq. is solved separately for each of the three Δ valleys. The resulting wavefunctions (Fig. 5) are then used to calculate 2D quantum density for each of the valleys. The 2D density is interpolated onto the 3D simulation domain to obtain a separate quantum correction potential for each valley.

We tested our new MC toolbox against experimental data for a 22 nm gate length GAA Si NW [1] with $\langle 110 \rangle$ channel orientation. The NW has elliptical cross-section with diameters of 11.3/14.22 nm, with effective diameter (elliptical circumference/π)D_{NW}=12.8 nm) and EOT = 1.5 nm. We reverse engineer the doping profile at the sub-threshold region at V_D= 0.05 V and V_D =1.0 V as shown in Figs. 1 and 2. We then simulated I_D-V_G characteristics of the 22 nm gate length GAA Si NW at both low and high drain biases using 3D SEQC MC toolbox without any free parameter with excellent agreement as can be seen in Fig. 3. We then scaled the Si GAA NW according to ITRS specifications to a gate length of 10 nm and EOT of 0.8 nm. Fig. 4 shows the I_D-V_G characteristics for the scaled 10 nm GAA NW at V_D=0.05 V and V_D=0.7 V predicted by the 3D FE SEQC MC. Table II collects all devices characteristics for Si GAA NW with gate lengths of 22 and 10 nm predicting that scaling to 10 nm gate will ensure superior electrostatic integrity and on-current performance of NW FETs.

To show how anisotropic QC can affect the I_D-V_G characteristics, we simulated two 8.1 nm gate length FinFETs, rectangular-like (REC) and triangular-like (TRI), with the $\langle 100 \rangle$ and $\langle 110 \rangle$ channel orientations, a channel perimeter of 26.5 nm, and area of 49.5 nm^2 (REC)/29.6 nm^2 (TRI), and EOT=0.55 nm. We have found (Figs. 6–9) that QC anisotropy effects play the strongest role in the $\langle 100 \rangle$ channel TRI device increasing the drain current by about 15% and slightly decreasing the current by 2% in the $\langle 100 \rangle$ channel REC device. The QC anisotropy has negligible effect in any device in the $\langle 110 \rangle$ orientation (see Table III).

REFERENCES

[1] S. Bangsaruntip et al., *IEDM Tech. Dig.*, pp. 526-529 (2013).
[2] J. Lindberg et al., *IEEE TED*, pp. 423-429 (2014).
[3] M. Aldegunde et al., *IEEE TED*, pp. 1561-1567 (2013).
[4] D. Esseni et al., "Nanoscale MOS Transistors: Semi- Classical Transport and Applications," Cambridge Univ. Press, 2011.
[5] B. Winstead et al., IEEE TED, 50, pp. 440-446, 2003.
[6] D. Nagy et al., *IEEE Trans. Nanotechnol*, pp. 93-100 (2015).

ISBN 978-0-692-50554-0

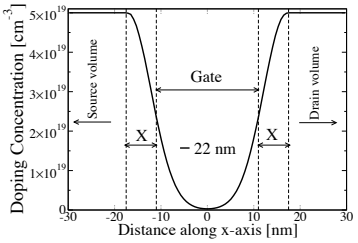

Fig. 1: Cross-section of Gausian-like doping profile along the transport x-direction for the GAA nanowire.

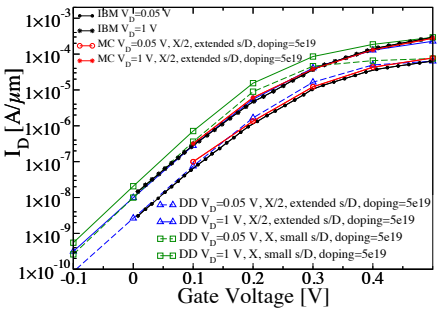

Fig. 2: Devising doping profile for the 22 nm GAA nanowire at V_D=0.05 V and V_D=1.0 V with DD simulations by changing the S/D region and the doping spread X, and a final MC simulation.

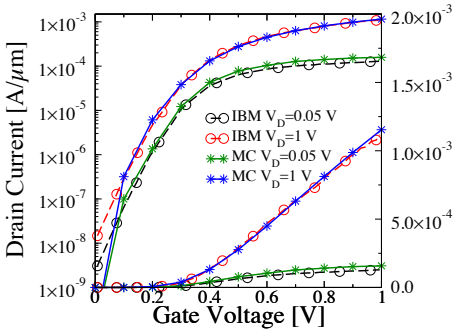

Fig. 3: I_D-V_G characteristics for the 22 nm GAA nanowire from the 3D FE MC with anisotropic SEQCs with no free parameter (full lines) compared against experimental data (dashed lines) [1].

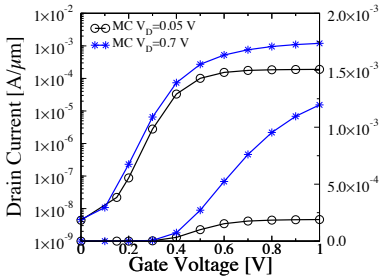

Fig. 4: I_D-V_G characteristics for the scaled 10 nm gate length GAA nanowire predicted by the quantum corrected 3D FE MC.

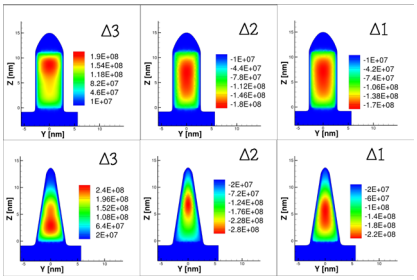

Fig. 5: The first wavefunctions for three Δ valleys, in the middle of the $\langle 100 \rangle$ channel for the REC (top) and TRI (bottom) cross-sections at V_G=0.8 V and V_D = 0.6 V.

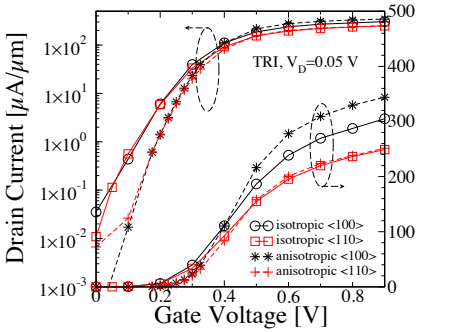

Fig. 6: I_D-V_G characteristics at V_D = 0.05 V for the TRI shape FinFET with the $\langle 100 \rangle$ and $\langle 110 \rangle$ channel orientations showing the effect of anisotropic SEQCs.

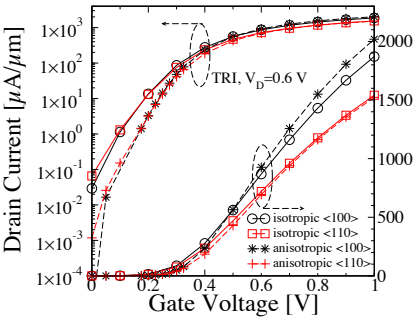

Fig. 7: I_D-V_G characteristics at V_D = 0.6 V for the TRI shape FinFET with the $\langle 100 \rangle$ and $\langle 110 \rangle$ channel comparing the effect of anisotropic SEQCs.

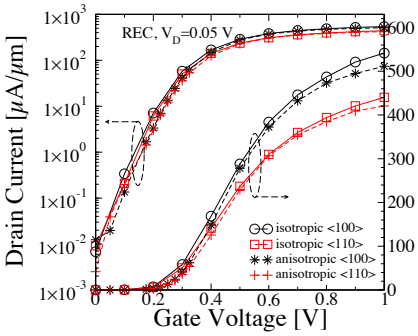

Fig. 8: I_D-V_G characteristics at V_D = 0.05 V for the REC shape FinFET with the $\langle 100 \rangle$ and $\langle 110 \rangle$ channel illustrating isotropic/anisotropic SEQCs.

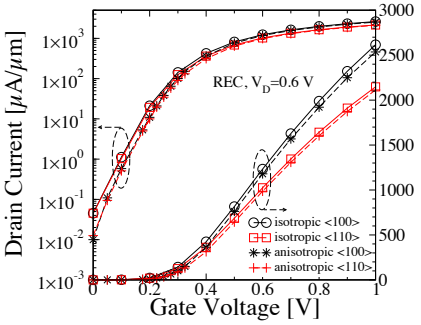

Fig. 9: I_D-V_G characteristics at V_D = 0.6 V for the REC shape FinFET with the $\langle 100 \rangle$ and $\langle 110 \rangle$ channel comparing isotropic/anisotropic SEQCs.

Orien-tation	Valley	ω_{yy}	ω_{zz}	m^*_{Tr}
$\langle 100 \rangle$	Δ1	$\frac{1}{m_t}$	$\frac{1}{m_t}$	m_l
$\langle 100 \rangle$	Δ2	$\frac{1}{m_l}$	$\frac{1}{m_t}$	m_t
$\langle 100 \rangle$	Δ3	$\frac{1}{m_t}$	$\frac{1}{m_l}$	m_t
$\langle 110 \rangle$	Δ1	$\frac{m_t+m_l}{2m_t m_l}$	$\frac{1}{m_t}$	$\frac{m_t+m_l}{2}$
$\langle 110 \rangle$	Δ2	$\frac{m_t+m_l}{2m_t m_l}$	$\frac{1}{m_t}$	$\frac{m_t+m_l}{2}$
$\langle 110 \rangle$	Δ3	$\frac{1}{m_t}$	$\frac{1}{m_l}$	m_t

TABLE I
THE EMT OF Δ VALLEY FOR $\langle 100 \rangle$ AND $\langle 110 \rangle$ CHANNEL ORIENTATIONS WHERE ω_{ij} =$1/m^*_{ij}$, ω_{yz} =0 AND DEGENERACY =2. WAFER ORIENTATION IS [100].

Gate length [nm]	22	10
V_T [V]	0.3	0.3
SS_{LOW} [mV/dec]	74	66
SS_{HIGH} [mV/dec]	77	67
DIBL [mV/V]	48	35
$DIBL_{MC}$ [mV/V]	64	39
I_{MC} [μA/μm]	1150	1196

TABLE II
V_T AND SUB-THRESHOLD SLOPE (SS) AT V_D = 0.05 V (LOW) AND 1.0/0.7 V (HIGH) FROM THE DD, DIBL FROM THE DD AND FROM THE MC, AND DRIVE CURRENTS (I_{MC}) AT V_G=1.0 V COMPARING 22 AND 10 NM GAA FETS.

FinFET	Rectangular		Triangular	
	iso	aniso	iso	aniso
V_T [V]	0.25	0.25	0.25	0.25
SS_{LOW} [mV/dec]	72		67	
SS_{HIGH} [mV/dec]	74		68	
$DIBL^{\langle 100 \rangle}_{MC}$ [mV/V]	82	76	70	48
$DIBL^{\langle 110 \rangle}_{MC}$ [mV/V]	84	77	77	51
$I^{\langle 100 \rangle}_{MC}$ [μA/μm]	2128	2075	1537	1667
$I^{\langle 110 \rangle}_{MC}$ [μA/μm]	1766	1728	1258	1251

TABLE III
V_T AND SS AT V_D = 0.05 V (LOW) AND 0.6 V (HIGH) FROM THE DD, DIBL FROM THE MC, AND DRIVE CURRENTS (I_{MC}) FOR REC AND TRI FINFETS COMPARING ISOTROPIC (ISO) AND ANISOTROPIC (ANISO) SEQCS.